

Multicomponent seismic polarization analysis

Saul E. Guevara and Robert R. Stewart

ABSTRACT

In the 3-C seismic method, the plant orientation and polarity of geophones should be previously known to provide correct amplitude information. In principle the linear polarization of waves can be used to determine the direction of the geophones and in that way field errors in location can be corrected. In this work, polarization information of two 3-C data set is analyzed with that purpose. The data are from a 3C-3D geophone directivity experiment and from a 3C-2D high-resolution data set. Two parameters were used to analyze polarization: the azimuth of horizontal receivers and the linearity. In the 3-D case, a first break window was used. In the 2-D case, first breaks and a second event were analyzed. For the first breaks, a relationship was found between polarization and direction source-to-receiver, but it is affected by many factors and the directional information cannot be inferred accurately from it. Effects like difference in response with the direction of the geophone were observed. The second event analyzed for the 2-D data, interpreted as an S refraction, presents much more definite linear polarization.

INTRODUCTION

The displacement of particles effected by elastic waves shows a preferred direction of polarization, depending on the seismic event that is causing the particle motion and on the elastic properties of the medium. This fact has been shown both theoretically and in many experiments. Polarization is related to shot-to-receiver orientation and to elastic properties of the medium.

Much effort has been devoted to take advantage of the polarization properties of waves. Some methods have been used successfully, mainly in earthquake seismology and in VSP. However in surface seismic exploration it is not so easily applied. This has been attributed to the heterogeneity of the near surface layers (Gal'perin, 1977) and likely the coupling and response of the 3-C geophone. A drawback of polarization analysis is that it is difficult to discriminate because the seismic events usually are mixed.

Polarization of seismic events is not an issue in the conventional seismic method, where only vertical ground motion is measured, but should be taken in account in multicomponent seismic method. In 3C-3D seismic processing geophone information should be rotated to the source-receiver direction to have a first polarization correction. Another rotation can be carried out to get information about anisotropy from the angles of the "natural coordinates", which are related to birefringence properties (Cary, 1994). Figure 1 illustrates the polarization characteristics in multicomponent 2-D and 3-D seismic acquisition. In 2-D, the components are oriented along the line defined by source and receiver. In 3-D, sources can be located at any direction with respect to receivers and so the energy can come from any direction.

Orientation of geophones is an important issue in 3C-3D seismic acquisition, because the processing depends on reliable information about geophone direction and polarity. Current techniques of acquisition generally keep all the geophones in the same predefined orientation such that all the axial and transverse components maintain the same polarity and direction. Such uniformity demands careful field deployment compared with conventional seismic exploration.

The most common geophone configuration in 3-C method is Cartesian, which consists of three orthogonal elements, two horizontals, axial and transverse, and one vertical. Figure 2 shows the 3-C geophone configuration used to acquire the data examined in this work. A test of the response of this type of geophone was carried out by Lawton and Bertram (1993).

Use of polarization information of first arrivals to get geophone orientation for 3-C seismic method is also found in Bland and Stewart (1996). As pointed out there, there are geometrical and polarity errors, like location of sources, location of geophones, direction of geophones and incorrect wiring, that could be identified with this method. However the results gave low correlation between polarization and direction. The interest in investigating that problem was a major reason to carry out the geophone direction experiment in Shaganappi 3C-3D.

The goal of this work is contributing to the development of a procedure to determine the direction of the source and the orientation of the receiver, from the seismic event's polarization of 3C-3D seismic data. Also contributing to analyze the azimuthal effect on polarization in real data.

Data from a geophone orientation experiment in Shaganappi 3C-3D is used here. Also 3C-2D data from a high-resolution survey over the Blackfoot field is analyzed.

METHODOLOGY

Three methods are used here to analyze the two seismic datasets: hodograms, histograms and the covariance matrix method. Hodograms allow a visual analysis, and angle of direction and linearity were measured with the other two methods.

Hodograms are useful ways to show the polarization information. A hodogram is the curve described by the displacement of two components over a specific time window. They are a description of the particle trajectory. A hodogram is illustrated in Figure 3(b).

Histograms of the two components resultant with respect to azimuth, have been used successfully in VSP method to calculate orientation of geophones from polarization information. The method used here was developed by DiSiena et al. (1984). Azimuth angles are classified into a number of classes and each resultant is added to its class. The outcome is a histogram with information about direction and linearity of polarization. It is illustrated in Figure 3(c). Each component is located at the origin, and the azimuth is measured having as a reference one of them. In this work the references are H1 in 3C-3D and R in 3C-2D. Because of the features of the

program used, in this work the azimuth direction is clockwise for 3C-3D and counter-clockwise for 3C-2D.

Montalbetti and Kanasevich (1970) present a method using a covariance matrix of multi-component data to analyze and filter polarized waves from earthquakes. In two dimensions, given components H1 and H2, the covariance matrix is given by:

$$V = \begin{pmatrix} \text{var}[H1] & \text{cov}[H1, H2] \\ \text{cov}[H1, H2] & \text{var}[H2] \end{pmatrix}$$

An estimate of the rectilinearity of the particle motion trajectory over a specific time window can be established from the diagonalization of the matrix. The resultant two eigenvalues give information on the circularity or linearity of the data set. If λ_1 is the largest eigenvalue and λ_2 the shortest, the ratio λ_2/λ_1 gives the circularity of the data. So we can define a quantity f :

$$f = 1 - \frac{\lambda_1}{\lambda_2}$$

which gives the linearity of the trajectory. If f is close to 1 the polarization is linear, if f is close to 0 the polarization is circular, and for intermediate quantities it is elliptical.

ANALYSIS OF THE DATA

First break windows from the two data sets were analyzed. The first breaks correspond to direct and refracted P waves, which are linearly polarized in the wave direction of propagation for an isotropic and homogeneous medium. The first arrivals have the advantages of being easily distinguished, not mixed with other events, and the effect of geology on the wave should be small. Also a second event was analyzed for the 3C-2D data. The data were analyzed without any filtering or amplitude correction.

The main topics were:

1. Check for relation between polarization in first breaks and azimuth source-receiver.
2. Comparison of polarization of first break window with a second seismic event.
3. Check dependence of polarization with direction of receiver and with offset.
4. Effect of the choice of the window and band pass filtering.

Shaganappi 3C-3D field experiment

The Shaganappi 3C-3D seismic survey was acquired at the west end of University of Calgary campus. For a complete description see Bland et al. (1998). It covered an

area of 320 by 210 m. The source used was two 450 Kg IVI mini-vibrators synchronously sweeping from 8 to 128 Hz.

In order to perform the orientation experiment, a cluster of nine 3-C geophones with varying orientations was located at a central point. The source and geophone locations are shown in Figure 4 and the geophone spread is shown in Figure 5. Sources and receivers are identified by the numbers in those figures. The direction of the geophones is defined by the arrows in Figure 5. The receivers are located in an area smaller than 1 m².

Table 1 has the azimuth of the geophone directions (H2). The geophones distribution and direction was calculated over photographs using a photogrammetric technique.

Table 1: Azimuth of geophone direction in the experiment

Geophone	1	2	3	5	6	8	9
Azimuth(°)	6	40	56	111	150	176	193

Part of a typical receiver gather is shown in Figure 6. In this figure the traces correspond mainly to the sources located in the northern half of the survey, and were detected by the H1 component of receiver 1. The first break window is also shown in Figure 6. That window was picked on the vertical component and was used in all of this analysis.

Figure 7 shows polarization in five receivers for the same shot. The source-to-receiver direction corresponds to the direction of receiver 1. Each row corresponds to a different receiver. The first column shows the hodogram of the vertical component against H1. The second column shows a hodogram of the two horizontal components. The third column shows a histogram for the two horizontal components. The value f in the third column corresponds to the parameter defined by the covariance matrix method. Theoretical polarization azimuth according to source location is shown with heads of arrow. Figure 8 corresponds to another shot in direction of receiver 1.

It can be noticed in Figure 7 that for the same seismic event (same shot, location of receivers and window) the polarization is different for each geophone. Then the polarization seems to depend on the geophone direction. This pattern of polarization is closely repeated in Figure 8: the shapes of histograms are similar, the least linearity is presented by receiver 5, and receiver 3 has high linearity.

Figure 9 shows the polarization analysis of the horizontal components for six shots with approximately the same direction as receiver 1 (difference lesser than 2°). Source 155 is the closest to receiver 1 (approx. 20 m) and source 9 is the farthest (approx. 150 m). Notice that the polarization angle seems to change with the offset, and it is not 90° as expected.

Figure 10 shows the polarization in six receivers for the same shot with came from a location in the direction H2 of receiver 5. As in figures 7 and 8, the polarization

depends on the geophone. However the histograms pattern is different: receivers 5 and 6 have the highest linearity and receiver 3 and 8 the lowest. If the low linear polarization of receiver 5 in figures 7 and 8 were due to coupling or other particular problems of the geophone, probably there were the same problem in Figure 10. It can be noticed that geophones 1 and 5 are almost orthogonal (table 1).

Figure 12 is an example to analyze the effect of filtering and size of window. The data corresponds to single shot and receiver. The first row shows the standard data, without filtering, the second row shows the data with a 10-60 Hz band pass filter and the third row corresponds to a smaller window, defined as the upper half of the original window. The columns are the same as in Figure 7. Filtering provides a smoother hodogram, and higher linear polarity but the angle measured in the histogram remains closely the same. Reducing the window size can affect strongly the dominant direction and the shape of the hodogram.

3C-2D data from Blackfoot III

The same methodology was applied to data from a 3C-2D seismic survey, Blackfoot III. This was an experimental survey recorded in 1997 in the Blackfoot area (Alberta, Canada), by the CREWES Project (Hoffe et al, 1998). It included many types of seismic data. A high-resolution seismic line with a length of 1 km and distance between geophones of 2 m was carried out, and a shot gather of this line was chosen for the test. The signal/noise relation is higher than in Shaganappi 3C-3D.

The shot point is offset from the geophone line by 48 m, so there is a 3-D effect. Dynamite was the source of energy, with a depth of 18 m and a charge size of 4 kg. There were 171 receivers almost symmetrically distributed relative to the source of energy. Figure 11 illustrates the spread. Two windows were chosen to perform the analysis. One window for first arrivals, with apparent velocity of 2300 m/s, and the other for a second event, with apparent velocity close to 800 m/s. Figure 13 displays in true amplitude the first 700 ms of data for each component and the two windows.

The two horizontal components in 2-D are called radial (R) and transverse (T), radial in the direction of the line and transverse perpendicular to it. The vertical component is identified with V. According to the deployment of the geophones, radial corresponds to component H2 in Figure 1 (axial) and transverse to H1. The direction of the geophones is opposite the direction of ascending numbers in Figure 12. The azimuth in histograms is measured from R.

Six receivers distributed along the gather are analyzed in Figures 14 and 15. Figure 14 corresponds to the first breaks and Figure 15 to the second event. Each receiver corresponds to a row with three plots, identified with columns *a*, *b* and *c*. Column *a* shows hodograms of R against V, column *b* shows hodograms of the two horizontal components and column *c* shows the histogram of the two horizontal. The value *f* in *c* corresponds to the parameter defined by the method of covariance matrix.

The polarization of the first breaks (Figure 14) is weak in the horizontal component and strong in the vertical one, which, together with the apparent velocity, identify it as P refracted waves. The second event (Figure 15) shows strong linear

polarization in the horizontal components, and can be interpreted as a shear wave refraction because of its polarization and its apparent velocity (see Figure 13). A similar case is presented by Dufour and Lawton, (1996).

The case of the first arrivals window looks similar to the 3-D case: some correlation but low linearity and not clear direction results. There is some correlation between the dominant azimuth angles in data from the two windows (columns c in Figs. 14 and 15) but it is very weak.

In Figure 15 the most important characteristic of the second event is the high linear polarization in the horizontal components (Figures 15b and 15c and factor f). Table 1 shows the source-to-receiver azimuth according to the geometry of acquisition in Fig. 12, with its two values corresponding to opposite polarities. This result can be compared with Figure 13c. It can be noticed that there is a good correlation between the histogram and the results in the table. Receivers 75 and 95 show the lower polarity, which could be related with interference of ground-roll because they are closest to the source (see location in Figure 12), or with different response in orthogonal components.

Table 2: Azimuth according Geometry

Receiver Number	Offset	Azimuth
2	166.7	163.27 – 343.27
40	96.6	150.21 – 330.21
75	50.4	107.75 – 287.75
95	55.6	59.69 - 239.69
130	108.3	26.31 – 206.31
170	183.1	15.2 – 195.2

DISCUSSION OF RESULTS

1. In the 3C-3D first break analysis, the polarization azimuth doesn't agree with the azimuths source-to-receiver from calculations. In addition to that, the polarization has frequently low linearity. In the first break window of the 3C-2D data linearity seems even lower and the polarization angle doesn't agree with azimuth source-receiver. Those results agree with Bland and Stewart (1996) about the difficulties to obtain geophone direction from first arrivals using polarization.
2. The second window in 2-D data, interpreted as S refractions, shows clearly linear polarization, and the polarization azimuth has good agreement with the azimuth source-receiver.
3. The geophone response depends on the geophone direction in the 3C-3D data. The linearity appears higher if the axial component of the receiver is in the

direction of the source, and lower if the axial component is perpendicular to the source direction. The azimuth of polarization appears depending on the offset.

4. The choice of the window can have strong effect in the resulting angle and linearity. However a wide window that tries to include two cycles of the dominant frequency, shows consistent results in the case of vibrators, in spite of that the first breaks are not so clear. The first break window in the 2-D case are shorter and more difficult to define for the horizontal components. Band pass filtering affects the result, mainly the linearity.

Many factors, related to the source of energy, the receiver and the trajectory of the wave, could affect the polarization characteristics measured in this experiment. Factors related to the source are the signature, coupling, power, and location. Factors related to the trajectory are the structural and stratigraphic characteristics of the terrain, and its elastic properties as heterogeneity and anisotropy. Factors related to the receiver are its location and orientation, its coupling to the terrain, and the response characteristics of the geophones. Other factors that can affect the results are the environmental noise and the choice of the window.

The low agreement in the angles source-receiver and polarization at the 3C-3D data set can be related with geophones response. The photogrammetric technique used for measurement in the 3C-3D experiment is not very precise, and could contribute to error. The difference in geophone response can be related with electronic features of the instrument. Also geophone response depends on the azimuth and Poisson Ratio according to Kähler and Meissner (1983). An explanation to the low linearity in the first breaks could be the low energy (and low S/N relationship), in the horizontal receivers due to the almost vertical wave arrival. The geophone response could also cause this effect, especially in the low linearity for the transverse direction of the energy. Elastic properties could cause the change in the polarization angle with offset. The coupling of geophones and the environmental noise could contribute to those effects.

Taking in account the redundancy of data in 3C-3D method, it could be useful a statistical approach. That approach could take in account many factors that affect polarization, and also could get information about them. In that sense it would be related with seismic data inversion. More numerical analysis and new experiments have to be done to continue this study.

CONCLUSIONS

From the analysis of first arrivals polarization on a single geophone, the orientation of geophones cannot be consistently defined. A shear wave event in 2-D data gives a very clear linear polarization, which is correlated with the source-receiver direction. This event could be used to provide information of the geophones orientation in the field.

Some patterns of polarization with respect to direction of the receivers have been identified and future work could help to understand and, if it is possible, take advantage of them.

Identification of an event clearly polarized in the horizontal direction in 3C-3D could give more reliable information about orientation. That could be the case of shear wave refractions. However it could be difficult due to the difference in response with direction.

Many factors can affect the polarization results in 3C-3D seismic data. More work needs to be done understand their polarization characteristics for 3C-3D case. The patterns of the anomalies in polarization information could be related with other elastic parameters. A method to get reliable information on polarization in 3-D could be based on the multiplicity of the information, taking into account the high redundancy in 3C-3D seismic method

ACKNOWLEDGEMENTS

We thank Eric Gallant and Henry Bland for their valuable collaboration in many stages of this work, and Han-xing Lu and Brian Hoffe for their collaboration in the preparation of Blackfoot III and Shaganappi 3C-3D information. Also thanks to ECOPETROL from Colombia and the CREWES sponsors for their support.

REFERENCES

- Bland H. C., Lu, H. X., Stewart, R. R., Hoffe, B., 1998, The Shaganappi 3C-3D survey. CREWES research report, Vol. 10, 34-1.
- Bland H. C. and Stewart R. R., 1996, Geophone orientation, location, and polarity checking for 3-C seismic surveys. CREWES Research Report, Vol. 8, 3-1.
- Cary, P., 1994, 3D converted-wave seismic processing . CREWES research report, Vol. 6, 31-1.
- Dufour, J., Lawton, D., 1996, Refraction analysis of the Blackfoot 2D-3C data. CREWES Research Report, Vol. 8, 14-1 to 32.
- DiSiena, J. P., Gaiser, J. E., Corrigan, D., 1984, Horizontal components and shear wave analysis of three-component VSP data. in eds. Toksoz, N. and Stewart R. R. Vertical seismic profiling: advanced concepts. Geophysical Press.
- Gal'perin, E. I., 1977, The polarization method of seismic exploration. D. Reidel Publishing Company.
- Hoffe, B., Stewart, R. R., Bland, H. C., Gallant E. V, Bertram, M., 1998, The Blackfoot high-resolution seismic survey: design and initial results. SEG 68th Annual Meeting, Expanded Abstracts, 103-106.
- Kähler, S., Meissner, R. 1983. Radiation and receiver pattern of shear and compressional waves as a function of Poisson's Ratio. Geophysical Prospecting 29, 533-540.
- Lawton D., Bertram M. 1993. Field test of 3-component geophones. Canadian Journal of Exploration Geophysics, Vol 29, No. 1, 125-131.
- Montalbetti, J., Kanasewich E. 1970 Enhancement of teleseismic body waves with a polarization filter. Geophys. J. R. Astr. Soc., 21, 119-129.

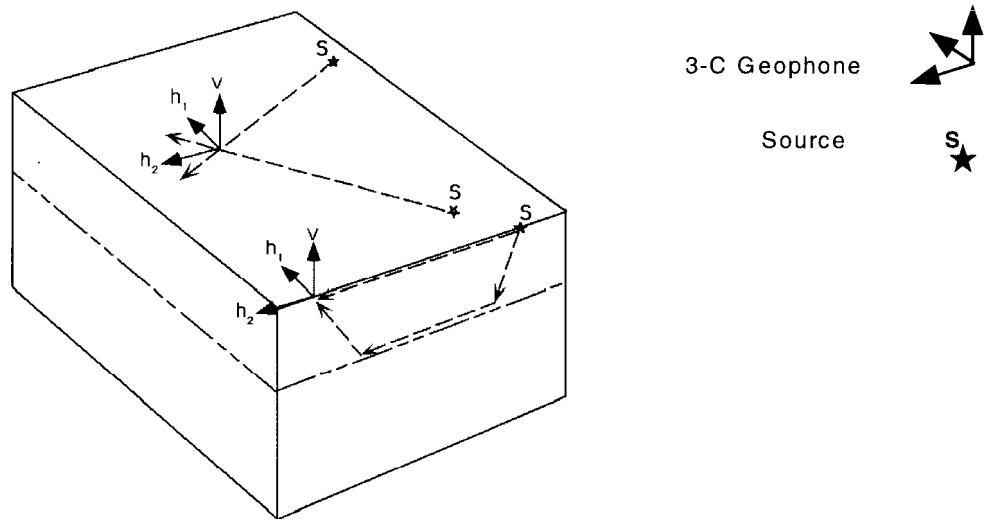


Figure 1. Orientation of geophones and polarization in 3C-2D and 3C-3D seismic surveys.

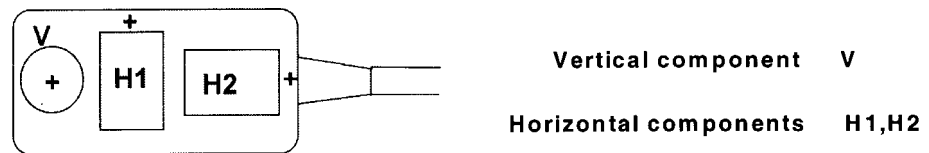


Figure 2. Top view of the elements and polarity of a 3-C geophone. The plus sign indicates the tap location that causes a positive value in the geophone output.

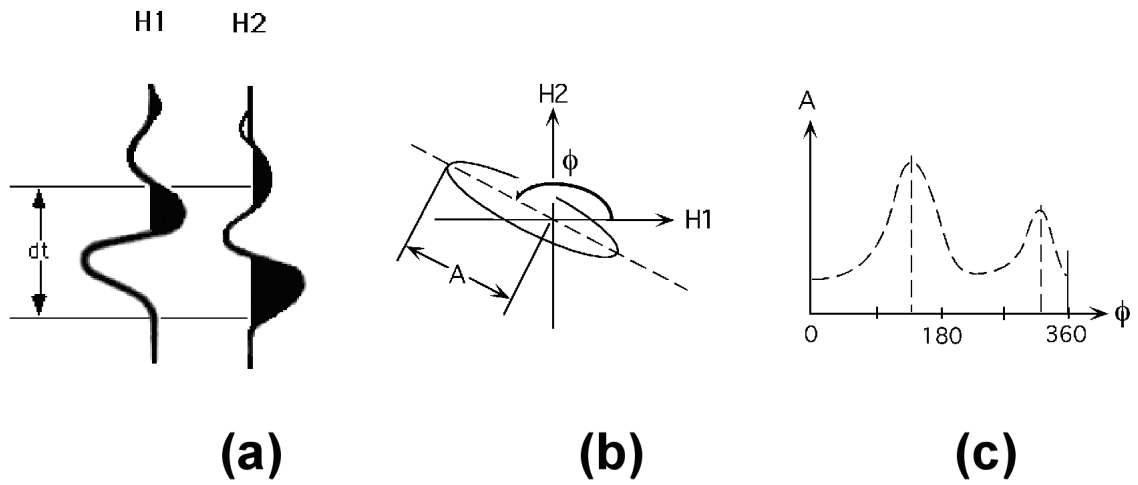


Figure 3. Methodology used to analyze polarization. (a) shows the two components and the analysis window. (b) is the corresponding hodogram and (c) is the histogram.

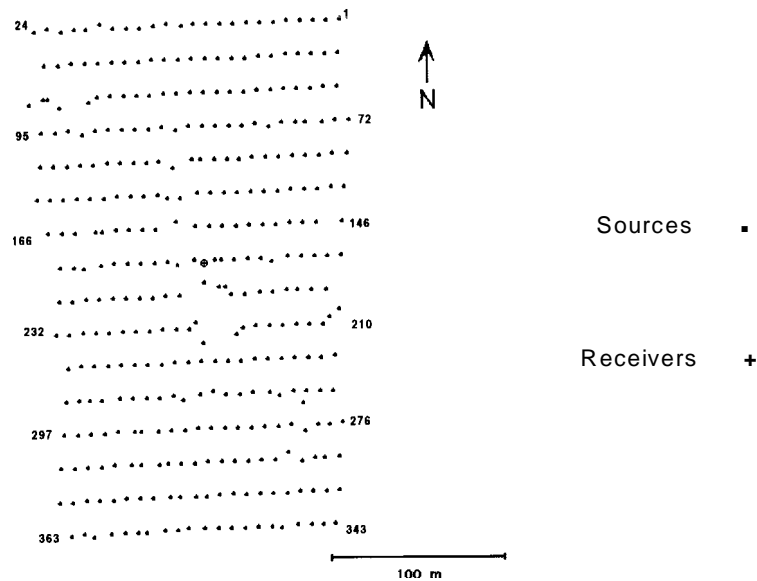


Figure 4. Source and receiver locations in the geophone orientation experiment at Shaganappi 3C-3D.

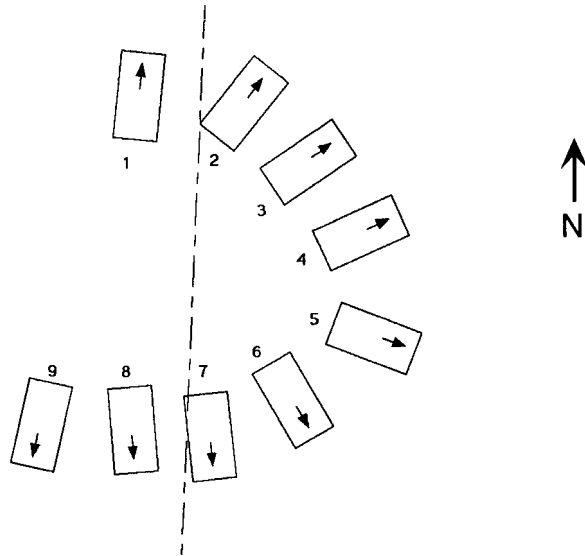


Figure 5. Geophone location in the experiment at Shaganappi 3C-3D. The arrows correspond to the component H2 plus sign in Figure 2. The dashed line joins two geophones and is used as a reference.

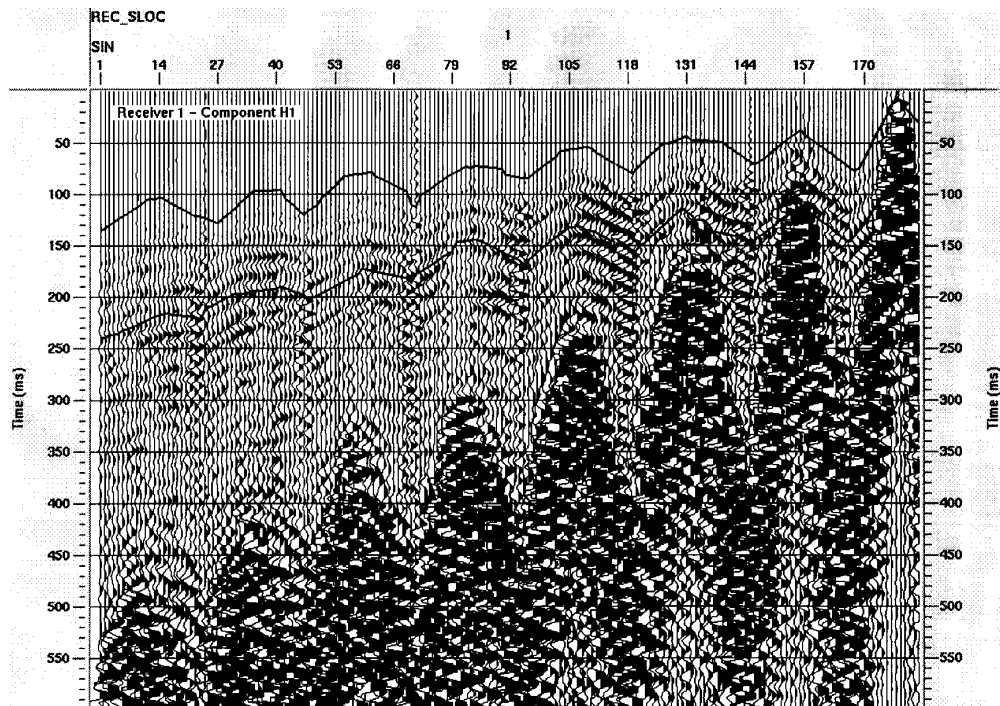


Figure 6. Example of data and window for the Shaganappi 3C-3D data. These traces corresponds to the northern shots recorded in the component H1 of the receiver 1.

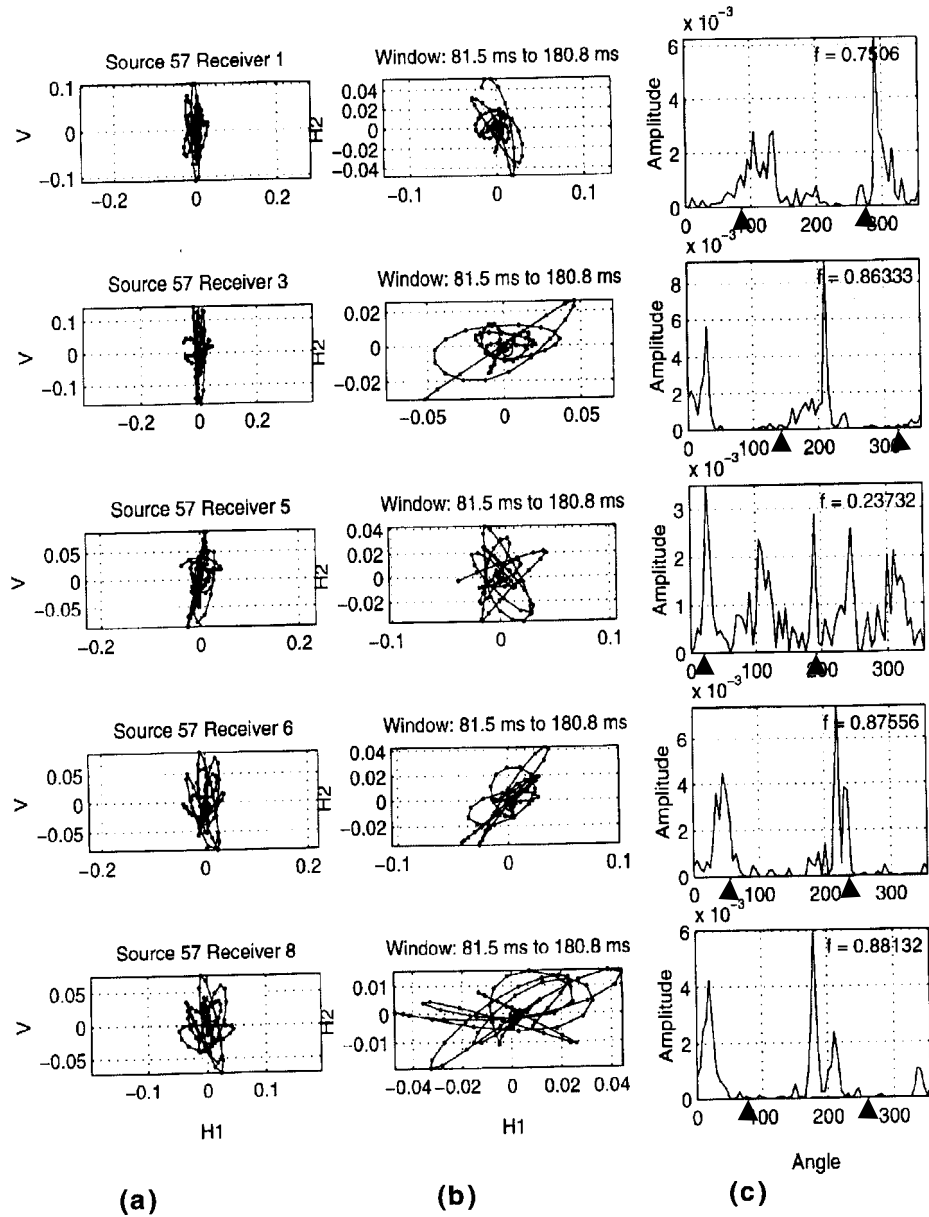


Figure 7. Polarization analysis for shot 57. The direction source-to receiver is the same that in Figure 8. Each row corresponds to a receiver. Receiver numbers correspond to Figure 5 and source to Figure 4. Column (a) are hodograms of vertical and H2 components, (b) are hodograms of the two horizontal components and (c) are the histograms and the linearity parameter f . The arrow heads show the theoretical polarization azimuth.

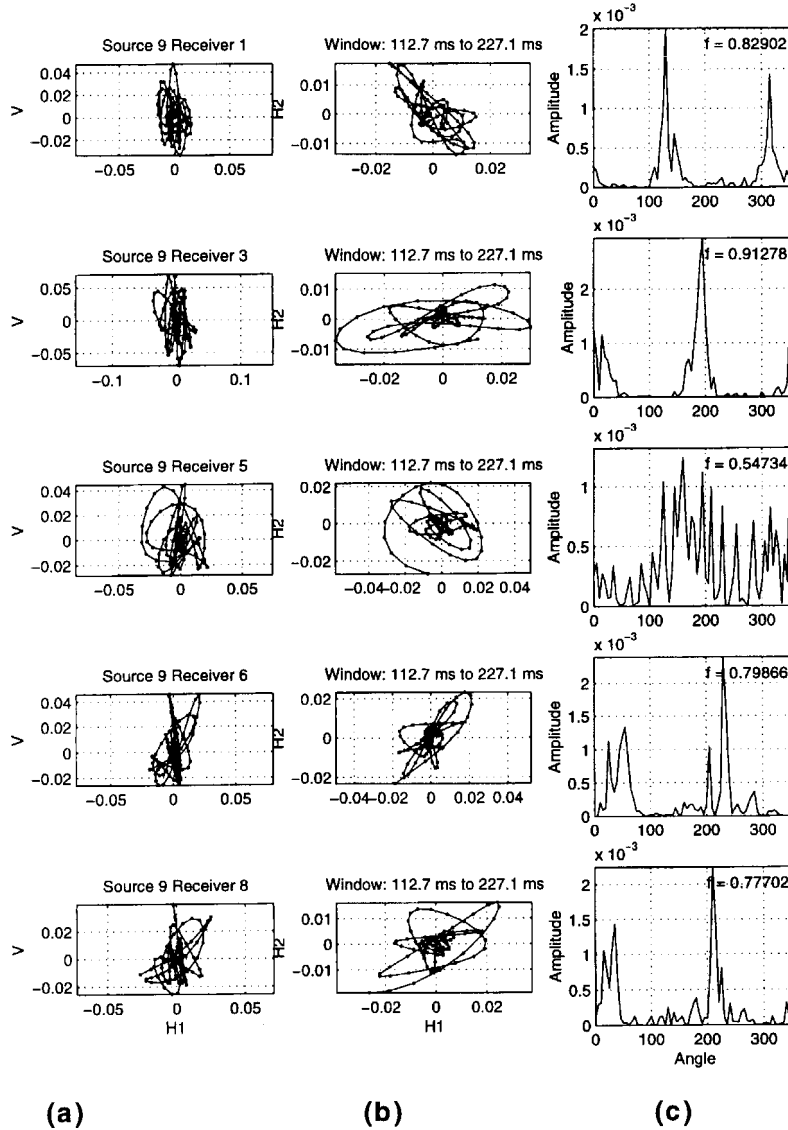


Figure 8. Polarization analysis for shot 9. The direction source-to receiver is the same that in Figure 7. Each row corresponds to a receiver. Receiver numbers correspond to Figure 5 and source to Figure 4. Column (a) are hodograms of vertical and H1 components, (b) are hodograms of the two horizontal components and (c) are the histograms and the linearity parameter f .

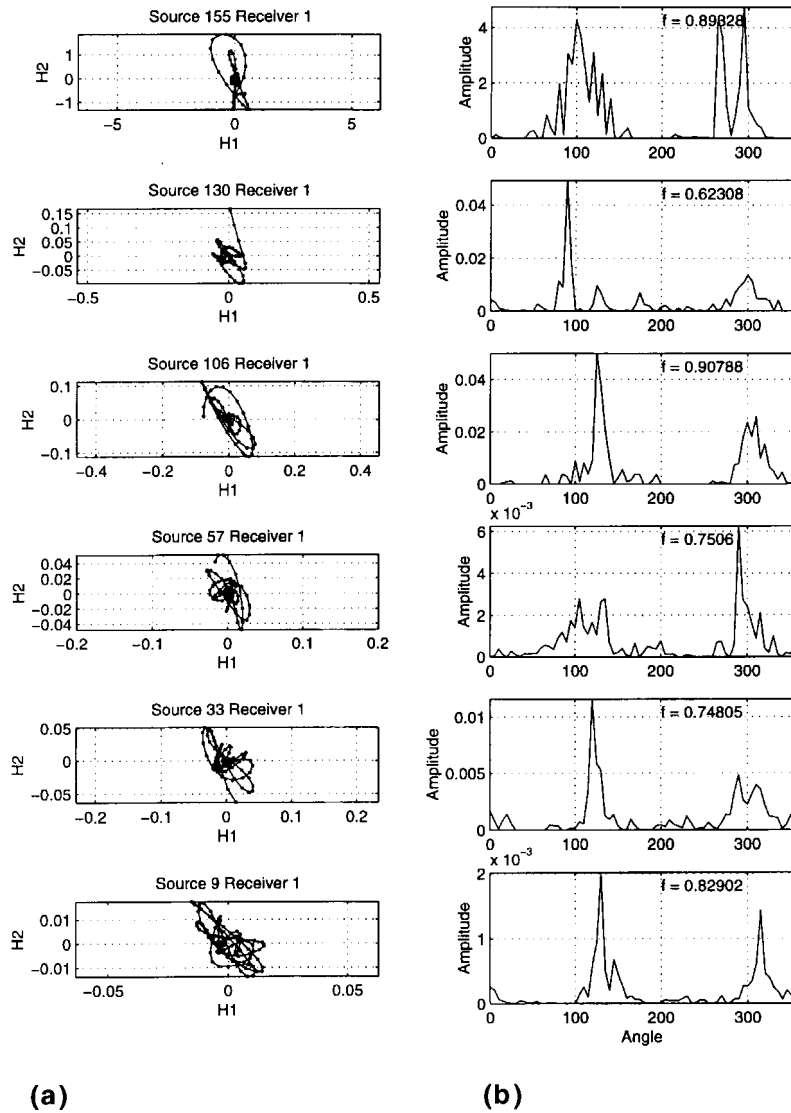


Figure 9. Polarization in the direction of receiver 1 for six source offsets. The shortest offset corresponds to the top row and the longest to the bottom. The column (a) is the hodogram for the horizontal components and column (b) is the histogram and the linearity parameter f .

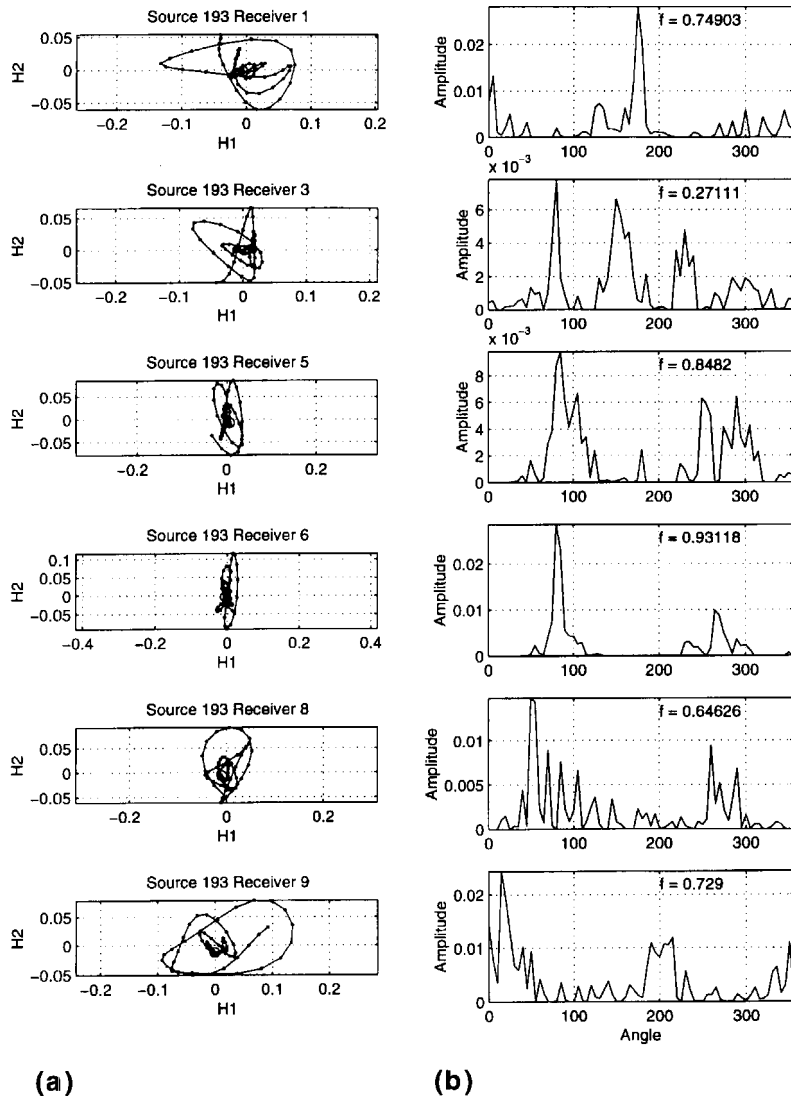


Figure 10. Shot with the direction of receiver 5 as detected by five receivers. Column (a) corresponds to the hodogram of the horizontal components and column (b) to the histogram and the linearity parameter f .

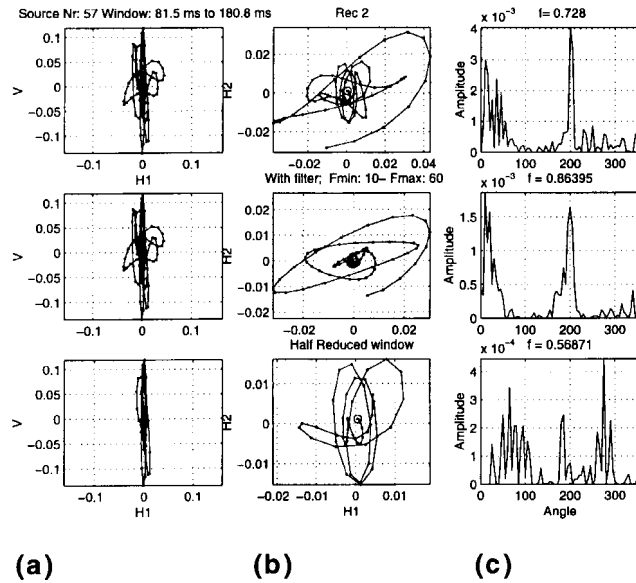


Figure 11. Polarization for a trace comparing filtering and size of the window. The first row corresponds to data without filter and with the standard window. In the second row a band pass filter 10-60 Hz was applied. In the third row the window is the upper half of the original. Column (a) corresponds to H1 and vertical, (b) to horizontals and (c) to histogram and the linearity parameter f .

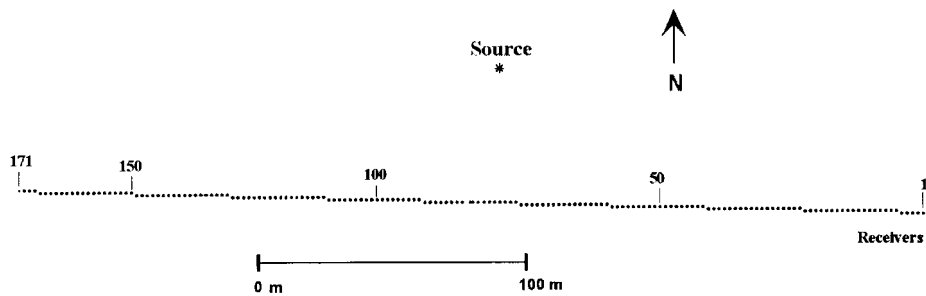


Figure 12. Source and receiver locations for the Blackfoot III data used.

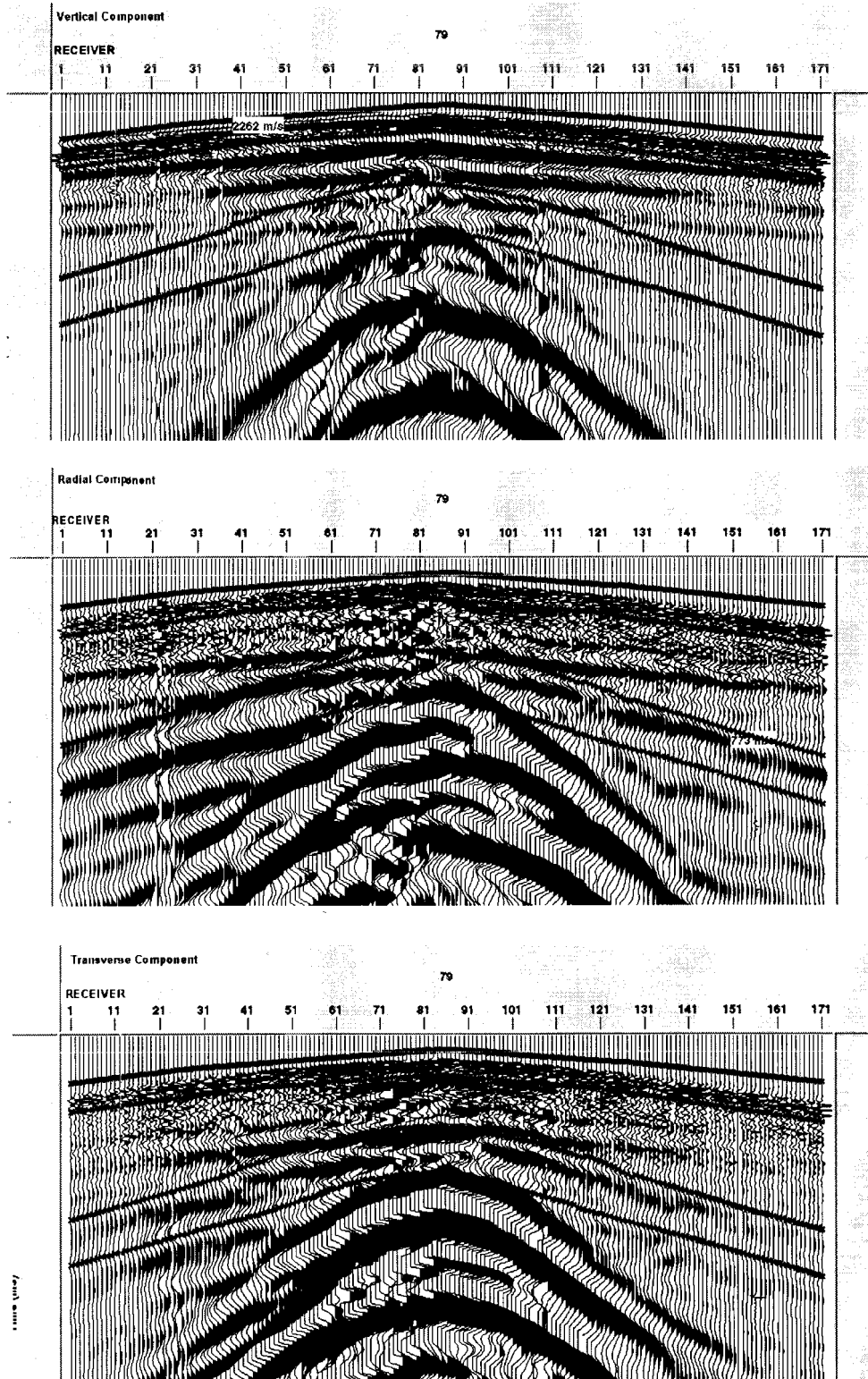


Figure 13. Three components and windows in a common shot gather from Blackfoot III.

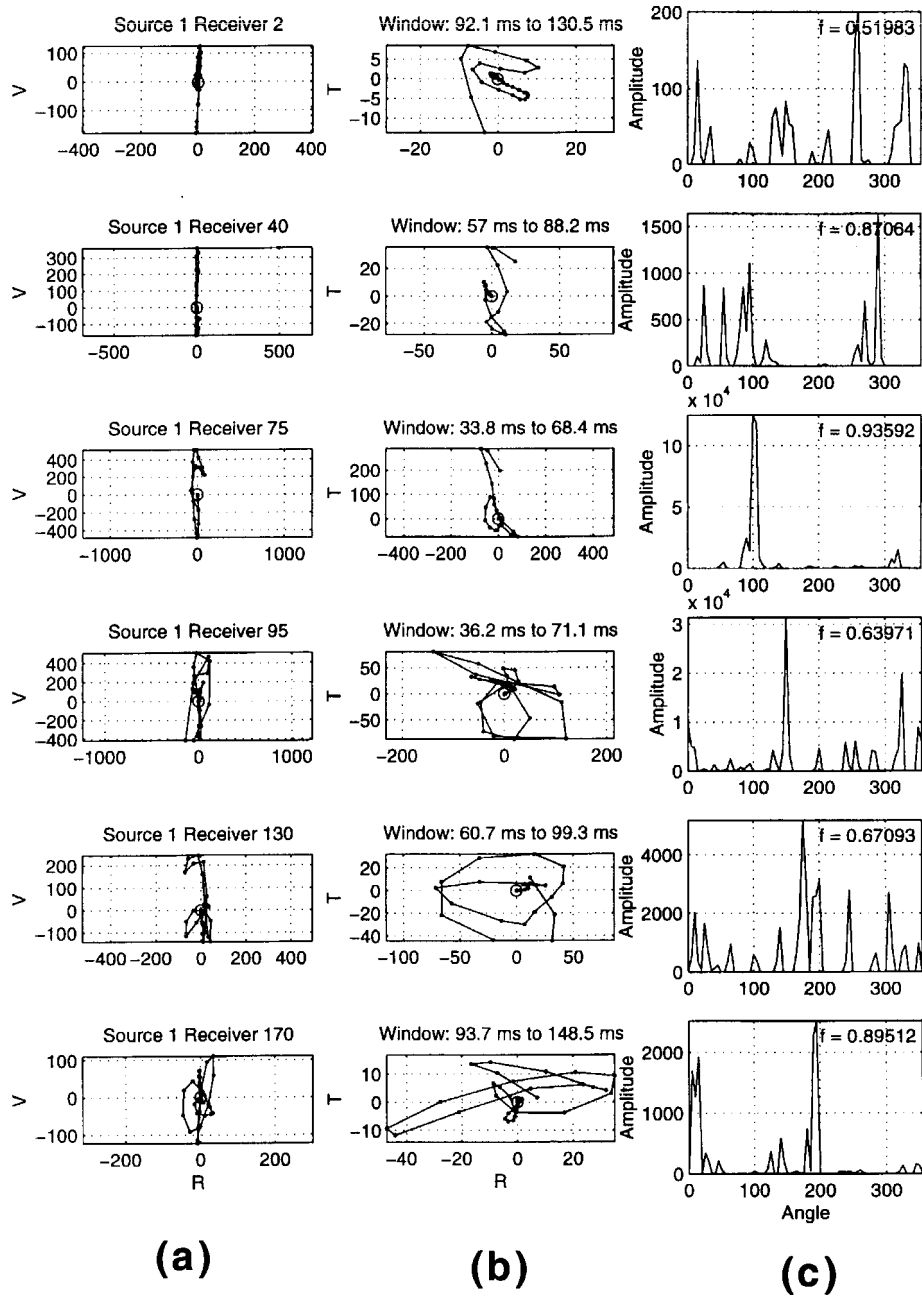
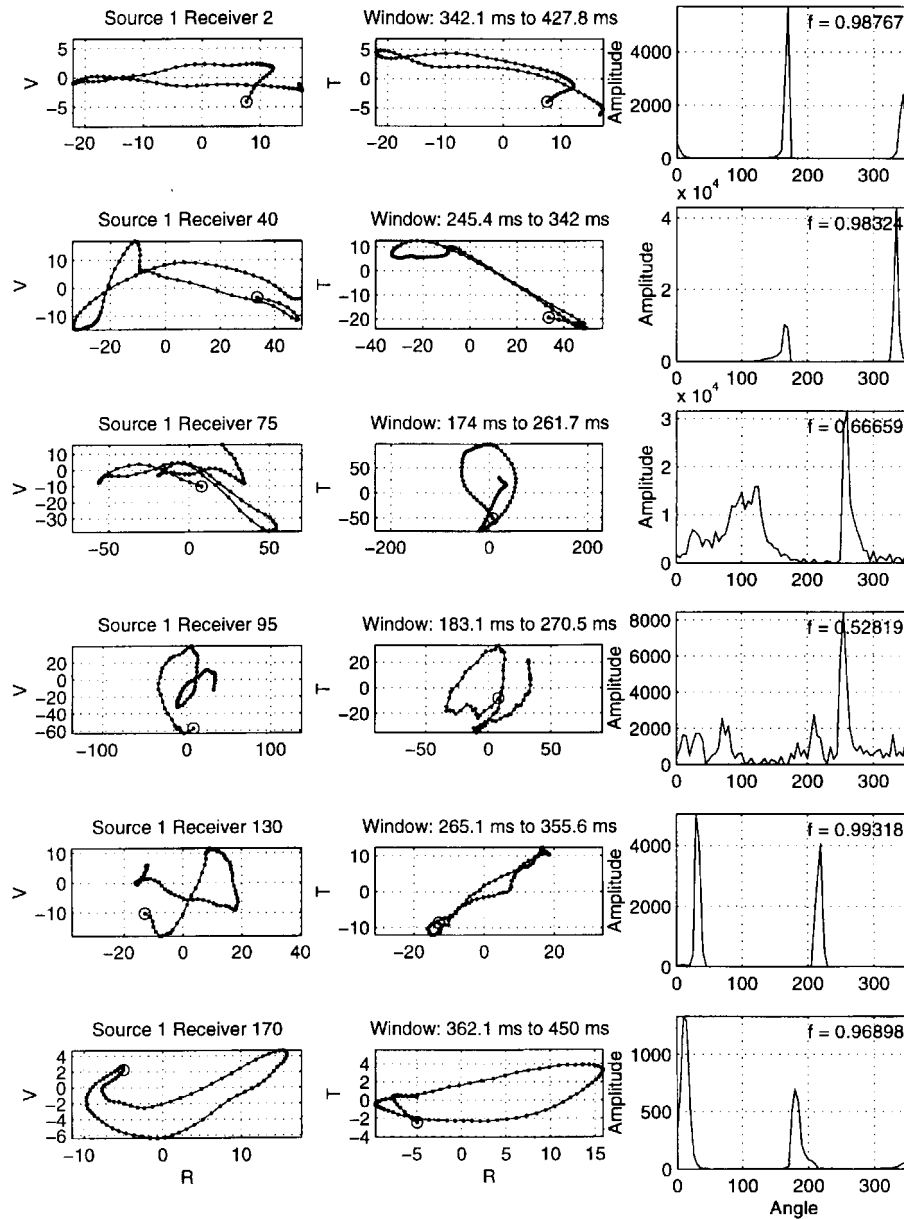


Figure 14. Polarization analysis for the first break window in Blackfoot III (3C-2D). Each row corresponds to a trace. Each row corresponds to a trace. Column (a) shows hodograms for radial and vertical components. (b) shows hodograms for the two horizontal components. (c) shows histogram for the horizontal and the linearity parameter f .



(a)

(b)

(c)

Figure 15. Polarization analysis in the second event of Blackfoot 3C-2D. Each row corresponds to a trace. Column (a) shows hodograms for radial and vertical components. (b) shows hodograms for the two horizontal components. (c) shows histogram for the horizontal and the linearity parameter f . Polarization is highly linear as shown by column (c).